distance scale, single reflections may be located to an accuracy of about 0.1 cm.

When obtaining a Smith chart display of reflections at a fixed frequency, instrument errors may be canceled by altering the differential gains of the difference amplifier to shift the point corresponding to a perfectly matched load (the center of the circle traced by a sliding load) exactly into the center of the screen.

VI. Summary

A swept-frequency instrument has been described, capable of producing either a visual or a permanent record of reflections along waveguide components or in space. Individual reflections in the range $|\Gamma| = 0.0005$ to full reflections may be indicated both in position and in magnitude and phase. There is no inherent upper frequency limitation to the technique; therefore instruments can be constructed to operate in any waveguide-size system. As a by-product, a single frequency or swept Smith chart display is available referred to a freely chosen plane.

Acknowledgment

The author wishes to thank Dr. D. L. Hollway and I. G. Morgan for their helpful discussions and P. W. Campbell, who manufactured the special waveguide components.

References

[1] D. L. Hollway and P. I. Somlo, "A high-resolution swept-frequency reflectometer," *IEEE Trans. Microwave Theory Tech.*, vol. MTT-17, Apr. 1969, pp. 185–188.
[2] D. L. Hollway, "The comparison reflectometer," *IEEE Trans. Microwave Theory Tech.*, vol. MTT-15, Apr. 1967, pp. 250–259.
[3] P. I. Somlo and D. L. Hollway, "Microwave locating reflectometer," *Electron. Lett.*, vol. 5, Oct. 1969, pp. 468–469.
[4] J. Detlefsen, "Frequency response of input impedance implies the distribution of discontinuities of a transmission-line system," *Electron. Lett.*, vol. 6, Feb. 1970, pp. 67–69.
[5] D. P. Franklin, "Hypotenuse function generator," *Electron. Eng.* (London), vol. 41, Jan. 1969, pp. 63–65.
[6] D. L. Hollway, "An improved hypotenuse function generator," to be published.
[7] H. A. Gebbie, C. F. Osborne, N. W. B. Stone, and B. K. Taylor, "The NPL teramet," *Engineer* (London), Oct. 1968.
[8] C. E. Muehe, "Band-pass time-domain reflectometry," *IEEE Int. Conv. Rec.*, 1969, pp. 416–417.
[9] Hewlett-Packard Co., "Narroband TDR locates waveguide faults," *Microwave J.*, vol. 13, Dec. 1970, p. 16.

Theory and Operation of a Reciprocal Faraday-Rotation Phase Shifter

WILLIAM E. HORD, MEMBER, IEEE, FRED J. ROSENBAUM, SENIOR MEMBER, IEEE, AND JAMES A. BENET, MEMBER, IEEE

Abstract—**The operation of a longitudinally magnetized fully filled square-waveguide reciprocal-ferrite phase shifter is described. The frequency characteristics of the phase shifter are predicted and measured. An error analysis, including rotational errors incurred in wide-band operation and manufacturing tolerances, is used to predict the loss performance of the device. The effect of the ferrite parameters and the waveguide geometry on phase-shifter performance may be calculated using this analysis. The variation of the phase shift with temperature as well as high-power effects are presented, and design considerations, including choice of ferrite saturation magnetization for wide-band performance, are discussed. Experimental results closely confirm the key aspects of this theory.**

Manuscript received December 22, 1970; revised June 6, 1971.
W. E. Hord is with the Department of Engineering, Southern Illinois University, Edwardsville, Ill. 62025, and the Emerson Electric Company, St. Louis, Mo.
F. J. Rosenbaum is with the Department of Electrical Engineering, Washington University, St. Louis, Mo., and is a Consultant to the Emerson Electric Company, St. Louis, Mo.
J. A. Benet is with Spartan Manufacturing Company, Flora, Ill.

I. Introduction

ALTHOUGH ferrite-loaded waveguiding structures have long been used as phase-shifting elements [1]–[7], design procedures for reciprocal phase shifters have remained largely empirical. The principle reason is that the ferrite–microwave field interaction in many useful phase-shifter geometries cannot be calculated exactly. An excellent example is the Reggia–Spencer device in which a longitudinally magnetized ferrite

rod inhomogenously loads a rectangular waveguide. Recently, however, approximation procedures have been developed which provide results sufficiently accurate so that useful design information for certain simple waveguide cross sections can be obtained [8]–[10]. It is our purpose in this paper to analyze the operation of a fully loaded square cross-section Faraday-rotation reciprocal phase shifter and to present design criteria for this device.

A saturated ferrite may be described by a scalar relative permittivity ϵ_f and a tensor permeability [11]

$$\boldsymbol{B} = \bar{\bar{\mu}} \cdot \boldsymbol{H} \tag{1}$$

$$\bar{\bar{\mu}} = \mu_0 \begin{bmatrix} \mu & -j\kappa & 0 \\ j\kappa & \mu & 0 \\ -0 & 0 & 1 \end{bmatrix} \tag{2}$$

where μ_0 is the permeability of free space. However, microwave phase shifters are generally operated with the ferrite partially magnetized [12]. At low levels of magnetization the relative permeability of the ferrite may differ appreciably from unity. To account for this Schlömann [13] has derived an expression for the isotropic $r-f$ permeability of a demagnetized ferrite

$$\mu_r = \frac{2}{3}\left[1 - \left(\frac{\omega_m}{\omega}\right)^2\right]^{1/2} + \frac{1}{3} \tag{3}$$

where

ω microwave radian frequency;
ω_m magnetization frequency $((2\pi\gamma)(4\pi M_s))$;
γ gyromagnetic ratio (2.8 MHz/Oe);
$4\pi M_s$ saturation magnetization.

In this discussion partial magnetization of the ferrite will be assumed. The tensor permeability of (2) will be multiplied by the scalar μ_r and the elements of the tensor will be taken to be

$$\mu \approx 1$$

$$\kappa \approx \left(\frac{4\pi M_r}{4\pi M_s}\right)\left(\frac{\omega_m}{\omega}\right)$$

where $4\pi M_r$ is the level of magnetization existing in the ferrite. Variable phase shift is obtained by changing the value of $4\pi M_r$ in the ferrite.

For a plane-wave propagating in an infinite ferrite medium along the direction of the applied magnetic field, the normal modes of propagation are right and left circularly polarized waves having different propagation constants [14]:

$$\beta_\pm = \beta\sqrt{\mu_r\epsilon_f}\,[\mu \pm \kappa]^{1/2}. \tag{4}$$

Here $\beta = \omega/c$ is the free-space propagation constant, c is the speed of light in vacuo, and ϵ_f is the relative dielectric constant of the ferrite.

Consider a linearly polarized wave at some point in the ferrite. This wave can be decomposed into two symmetrical contrarotating components. After propagating a distance l, the linearly polarized wave will have its plane of polarization rotated through an angle θ due to the Faraday effect. The Faraday rotation per unit length is given by

$$\frac{\theta}{l} = \frac{1}{2}(\beta_- - \beta_+). \tag{5}$$

The wave will also undergo a phase shift of

$$\frac{\phi}{l} = \frac{1}{2}(\beta_- + \beta_+). \tag{6}$$

Faraday rotation also may be observed in waveguide structures that support cross-polarized propagating modes.

To demonstrate the effect of the waveguide cross section on a Faraday rotator, consider a square waveguide $(a \times a)$ completely filled with ferrite. It can be shown that the normal modes are again right and left circularly polarized waves having propagation constants approximately given by [9]

$$\beta_\pm = \beta_0\sqrt{\mu_r\epsilon_f}\left[\mu \pm \frac{8}{\pi^2}\kappa\right]^{1/2} \tag{7}$$

where

$$\beta_0 = \omega\sqrt{\mu_0\epsilon_0}\left[1 - \left(\frac{\omega_c}{\omega}\right)^2\right]^{1/2} \tag{8}$$

and

$$\omega_c = \frac{\pi}{a\sqrt{\mu_r\epsilon_f}\sqrt{\mu_0\epsilon_0}}. \tag{9}$$

The boundary conditions imposed by the waveguide decrease the amount of Faraday rotation per unit length relative to the infinite ferrite medium by

$$\frac{\theta_{\text{sq wg}}}{\theta_{\text{inf}}} = \frac{\left[1 - \left(\frac{\omega_c}{\omega}\right)^2\right]^{1/2}\left[\sqrt{\mu + \frac{8}{\pi^2}\kappa} - \sqrt{\mu - \frac{8}{\pi^2}\kappa}\right]}{\sqrt{\mu + \kappa} - \sqrt{\mu - \kappa}}. \tag{10}$$

The factor $[1-(\omega_c/\omega)^2]^{1/2}$ is the dispersion associated with the waveguide, while $8/\pi^2$ is the coupling factor that accounts for the transverse variations of the field distributions. In a similar analysis for the completely filled circular waveguide, Severin [15] obtains a coupling factor of 0.83. Thus equivalent coupling factors are exhibited by both square and circular ferrite-filled waveguides.

II. Phase-Shifter Analysis

Various versions of the reciprocal Faraday-rotation phase shifter have been described in the literature [12], [16], [17]. This paper will be concerned with the analy-

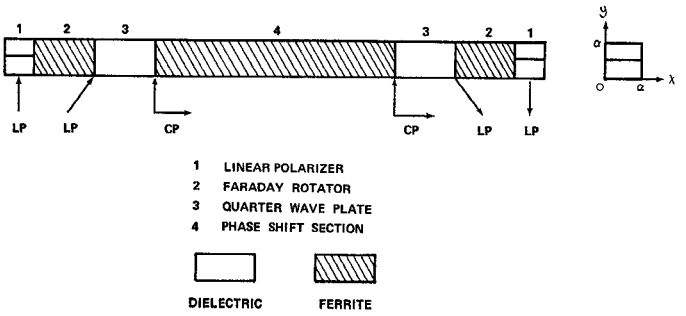

Fig. 1. Phase-shifter geometry.

sis of the phase shifter shown in Fig. 1. The ferrite and dielectric sections are glued together and directly metallized to form a waveguide. The permittivity of the dielectric material is chosen to match the ferrite permittivity closely. The Faraday rotator is magnetized to provide 45° rotation to a linearly polarized input wave. The quarter-wave plates are constructed by perturbing the square symmetry of that dielectric section so that a 90° time delay is provided for orthogonal linear fields. The linear polarizer consists of an absorbent vane which attenuates the mode whose E field lies in the plane of the vane. These elements are analyzed here and a transmission matrix describing the performance of the cascaded elements is formulated. The analysis treates only square waveguides of dimension $a \times a$.

The useful bandwidth of the phase shifter will be taken as that frequency range for which acceptable transmission losses are obtained. This bandwidth depends on the frequency dependence and interaction of the phase-shifter elements, principally the Faraday rotators and quarter-wave plates. These elements provide proper rotation and phasing only at their design frequency. At other frequencies rotational errors are introduced which result in elliptical polarization at the output port. The cross-polarized mode is absorbed in the output linear polarizer and hence a frequency-dependent insertion loss is generated. In order to design wide-band phase shifters with predictable performance, it is necessary to analyze these errors.

A. Faraday Rotator

A simplified model of the Faraday rotator consists of an infinitely long dielectric waveguide loaded by a ferrite section of length l. The ferrite length required to provide 45° of rotation at the design center frequency ω in a given ferrite material may be found from (5) and (7)–(9) with the result

$$l_{FR} = \frac{\frac{\pi}{2}}{\beta_0 \sqrt{\mu_r \epsilon_f}\left[\left(1 + \frac{8}{\pi^2}\kappa\right)^{1/2} - \left(1 - \frac{8}{\pi^2}\kappa\right)^{1/2}\right]}. \quad (11)$$

Here $\kappa \approx 2/3(\omega_m/\omega)$ since the Faraday rotators are axially magnetized to approximately 2/3 of the value of the saturation magnetization of the ferrite.

The transmission matrix describing the Faraday rotator may be found by following the analysis of Gurevich [16], who considered the transmission and reflection of plane waves normally incident on a logitudinally magnetized semi-infinite ferrite slab of length l, which is contained between two semi-infinite dielectric regions. For the square waveguide the normal modes in the ferrite are circularly polarized. There are two electric field transmission coefficients which are

$$T_{R\pm} = \frac{E_{\text{out}\,\pm}}{E_{\text{in}\,\pm}} = \frac{2\rho_\pm}{(1+\rho_\pm^2)\sin\beta_\pm l_{FR} - j2\rho_\pm \cos\beta_\pm l_{FR}} \quad (12)$$

where E_{out} and E_{in} are the E fields in the output and input waveguides which are fully filled with a dielectric medium ($\epsilon = \epsilon_d\epsilon_0$):

$$\rho_\pm = \frac{\beta_\pm}{\beta_d \mu_\pm} \quad (13)$$

and

$$\beta_d = \left[\omega^2\mu_0\epsilon_0\epsilon_d - \left(\frac{\pi}{a}\right)^2\right]^{1/2} \quad (14)$$

$$\mu_\pm = \mu_r\left[\mu \pm \frac{8}{\pi^2}\kappa\right] \quad (15)$$

with $\beta_\pm$ given by (7). To use the transmission coefficient of (13) the fields must be expressed in circularly polarized coordinates. Define $[T_{cp}]$ as the matrix which transforms linearly polarized coordinates to circularly polarized coordinates. Define $[T_{lp}]$ as the matrix which transforms circularly polarized coordinates to linearly polarized coordinates. Then, for the Faraday rotator

$$\begin{bmatrix} E_x \\ E_y \end{bmatrix}_{\text{out}} = [T_{lp}]\cdot[T_{FR}]\cdot[T_{cp}]\cdot\begin{bmatrix} 0 \\ 1 \end{bmatrix} \quad (16)$$

for an input field linearly polarized along the y direction. The matrix T_{FR} is defined by

$$[T_{FR}] = \begin{bmatrix} T_{R+} & 0 \\ 0 & T_{R-} \end{bmatrix}. \quad (17)$$

The input to the rotator is linearly polarized. The output is in general elliptically polarized since the transmission coefficients T_{R+} and T_{R-} are different.

The transmission loss of the Faraday rotator section is due to the reflections caused by the difference in the characteristic impedances of the ferrite- and dielectric-loaded waveguides. The total loss is found by evaluating

$$\text{transmission loss} = -10\log\left(|E_x|^2 + |E_y|^2\right) \quad (18)$$

using the normalized output amplitudes from (16). The loss is shown in Fig. 2. Notice that significant losses ($\approx$0.2 dB) can be expected below the design frequency for values of $k_m a \geq 0.45$.

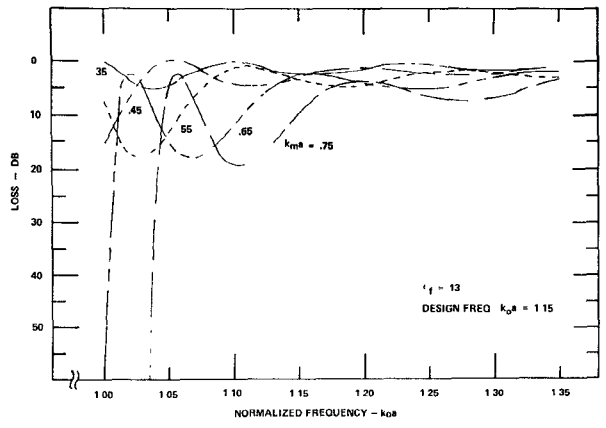

Fig. 2. Transmission loss of 45° Faraday rotator as a function of normalized frequency with $k_m a$ as parameters.

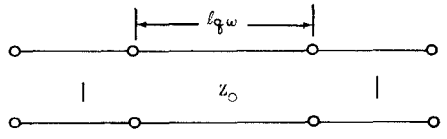

Fig. 3. Transmission line model of quarter-wave plate.

B. Quarter-Wave Plates

The quarter-wave plates may be constructed by removing a longitudinal section of length l_{qw} and depth δ, thus perturbing the symmetry of the square waveguide. The length of the cut from a given depth is

$$\frac{l_{qw}}{a} = \frac{\frac{\pi}{2}}{k_0 a\sqrt{\epsilon_d}\left\{\left[1 - \frac{\pi^2}{(k_0a)^2\epsilon_d}\right]^{1/2} - \left[1 - \frac{\pi^2}{(k_0a)^2\epsilon_d(1-\delta/a)^2}\right]^{1/2}\right\}}. \tag{19}$$

The depth of the cut should be small in order not to introduce appreciable discontinuity reactance at the junctions.

To calculate the transmission matrix of the quarter-wave plates, consider the equivalent transmission line shown in Fig. 3. The transmission coefficient for this circuit, neglecting the discontinuity reactance, is

$$\frac{E_2}{E_1} = \sqrt{1-\rho^2}\exp\left\{-j\left[\beta l_{qw} + \tan^{-1}\frac{\text{Im}\,(\rho)}{1+\text{Re}\,(\rho)}\right]\right\} \tag{20}$$

where

$$\rho = \frac{j(Z_0^2 - 1)\tan\beta l_{qw}}{2Z_0 + j(Z_0^2+1)\tan\beta l_{qw}}. \tag{21}$$

For the purposes of this analysis assume that the characteristic impedance of the waveguide is given by

$$Z_0 = \frac{\omega\mu_0}{\beta}\frac{b}{a} \tag{22}$$

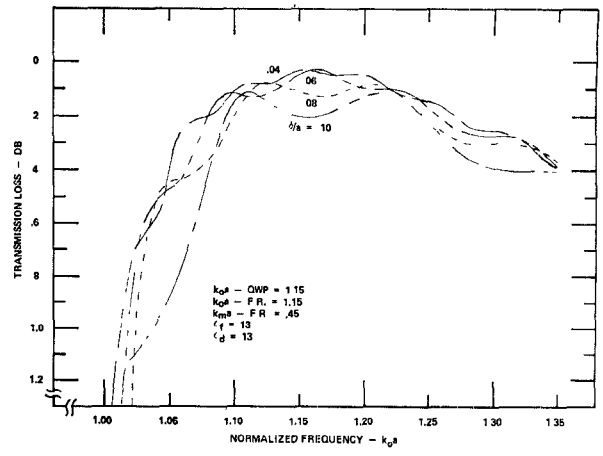

Fig. 4. Transmission loss of circular polarizer as a function of normalized frequency for various cut depths of the quarter-wave plate.

where b is the height of the waveguide and a is its width. If the cut is made so that the propagation constant of the horizontal mode (E_x) is delayed, the normalized characteristic impedances are

$$Z_{0x} = \frac{\left[(k_0a)^2\epsilon_d - \pi^2\right]^{1/2}}{\left[(k_0a)^2\epsilon_d(1-\delta/a)^2 - \pi^2\right]^{1/2}} \tag{23}$$

$$Z_{0y} = 1 - \delta/a. \tag{24}$$

Substitution of (23) or (24) into (20) and (21) results in transfer coefficients for the quarter-wave plates T_x or T_y.

If the input wave to the quarter-wave plate section is expressed in linearly polarized coordinates, the output wave is given by

$$\begin{bmatrix}E_x\\E_y\end{bmatrix}_{out} = \begin{bmatrix}T_x & 0\\0 & T_y\end{bmatrix}\begin{bmatrix}E_x\\E_y\end{bmatrix}_{in}. \tag{25}$$

C. Circular Polarizer

The tandem 45° Faraday rotator and quarter-wave plate combination sections produce the circularly polarized input required in the phase-shift section. This circular polarizer is nonreciprocal [19]. Assuming that reflections within this unit are small, the overall performance of the circular polarizer may be calculated by the matrix multiplication of (17) and (25) with appropriate conversion matrices inserted.

Fig. 4 shows the transmission loss versus frequency for a linearly polarized input to the Faraday rotator for different quarter-wave plate designs. The transmission was calculated by using only the desired sense of

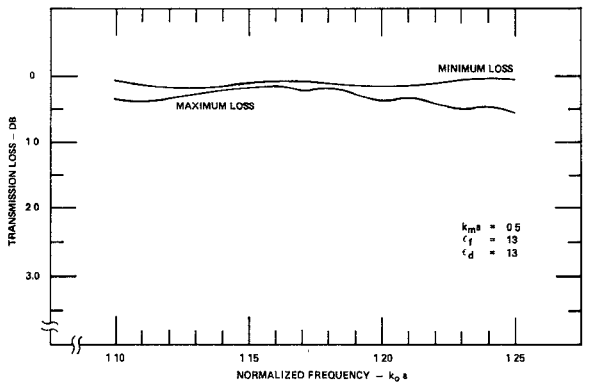

Fig. 5. Theoretical maximum and minimum insertion loss versus normalized frequency.

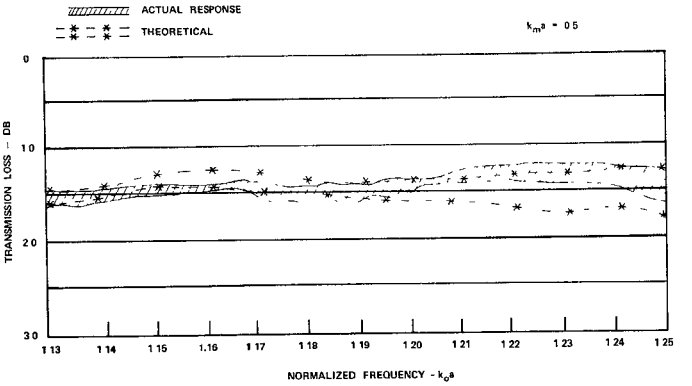

Fig. 6. Comparison of experimental and theoretical transmission loss of phase shifter.

circular polarization at the output port. The loss is caused by reflections and rotational errors which generate the opposite sense of circular polarization. From these curves it is seen that a circular polarizer with less than 0.3-dB loss over a 17-percent band can be easily obtained.

The circular polarization function can also be obtained using a uniform ferrite section by transversely magnetizing it with an appropriate quadrupole magnetic field. Excellent performance can be obtained in this way [16], [17].

D. Transmission Matrix Analysis of Phase Shifter

The performance of the phase shifter can be calculated by multiplying the transfer matrices of the individual components. The transfer matrix of the phase-shift section is given by (13) with l_{FR} replaced by the length of the phase shift section, l_{ps}, and $\beta_{\pm}$ calculated by (7) with κ set by the level of magnetization of the phase-shift section. Denoting this matrix by

$$[T_{ps}] = \begin{bmatrix} T_+ & 0 \\ 0 & T_- \end{bmatrix} \tag{26}$$

the overall frequency response of transmission through the phase shifter may be obtained by the matrix multiplication

$$\begin{aligned} \begin{bmatrix} E_x \\ E_y \end{bmatrix}_{out} = {} & [T_{lp}]\cdot[T_{FR}]\cdot[T_{cp}]\cdot[T_{qw}] \\ & \cdot[T_{lp}]\cdot[T_{ps}]\cdot[T_{cp}]\cdot[T_{qw}] \\ & \cdot[T_{lp}]\cdot[T_{FR}]\cdot[T_{cp}]\cdot\begin{bmatrix} E_x \\ E_y \end{bmatrix}_{in}. \end{aligned} \tag{27}$$

For a vertically polarized input the transmission loss is

$$\text{transmission loss TL} = -20\log\left|\frac{E_{y\,out}}{E_{y\,in}}\right|. \tag{28}$$

The magnitude of the cross-polarized component appearing at the output may also be calculated from (27).

Fig. 5 shows the theoretical transmission loss as a function of normalized frequency. At each frequency the maximum and minimum loss is found as the phase-shift section is incremented through the range of phase states. These results are compared with experimental data for several phase states in Fig. 6. The theoretical loss bounds were fitted to the experimental results at $k_0a = 1.13$. The deviation at midband is due to mismatch caused by the transitions used to match into the reduced cross-section phase shifter. The average loss level depends upon conductor and dielectric losses in the phase shifter and on fabrication procedures. Theoretical calculations predict approximately 1 dB for this average loss which compares well with the experimental results.

TABLE I
THEORETICAL AND EXPERIMENTAL DIFFERENTIAL PHASE SHIFT

k_0a	$\Delta\phi$ (DEGREES) THEO. *	$\Delta\phi$ (DEGREES) EXP. *
1.08	498	525
1.165	595	608
1.23	645	665

*$k_ma = 0.5$

A comparison of theoretical and experimental differential phase shift for several different frequencies is given in Table I. Note that the differential phase shift may be predicted with an accuracy of 5 percent.

III. DESIGN CONSIDERATIONS

The major advantage of the geometry selected is that the performance of the phase shifter can be readily calculated. The theoretical differential phase shift versus frequency for several ferrites is shown in Fig. 7, while Fig. 8 shows the maximum transmission loss due to rotational errors. As expected, the differential phase shift and the rotational loss both increase with increasing saturation magnetization. Thus for a prescribed bandwidth, a choice of ferrite can be made by reference to Fig. 8. The required phase shift is obtained by adjusting the length of the phase-shift section, l_{ps}.

The transmission loss shown in Fig. 5 was calculated

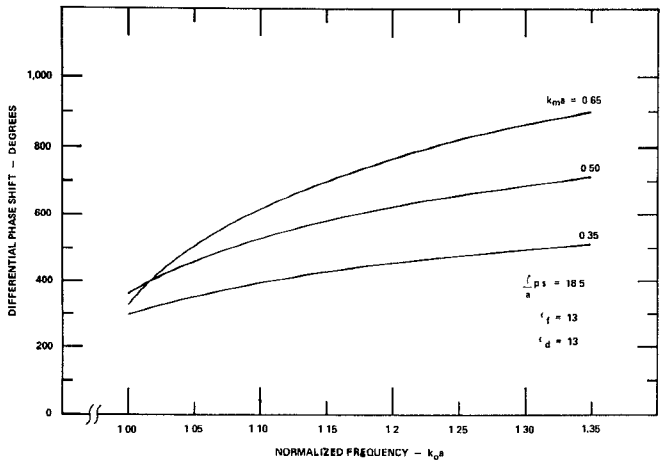

Fig. 7. Theoretical differential phase shift as a function of normalized frequency for various ferrites.

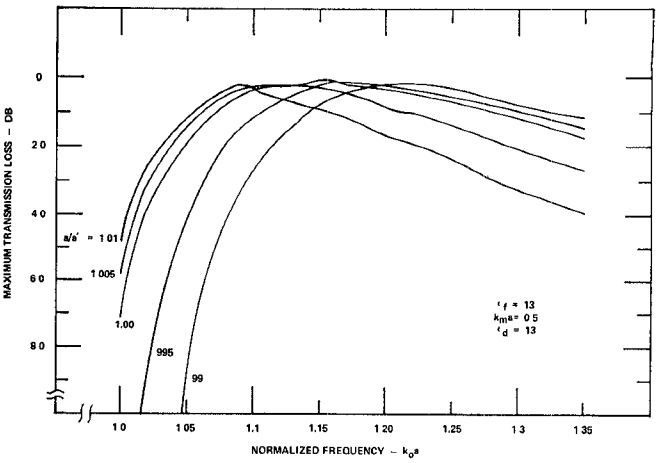

Fig. 9. Maximum transmission loss as a function of normalized frequency for various waveguide aspect ratios (a/a').

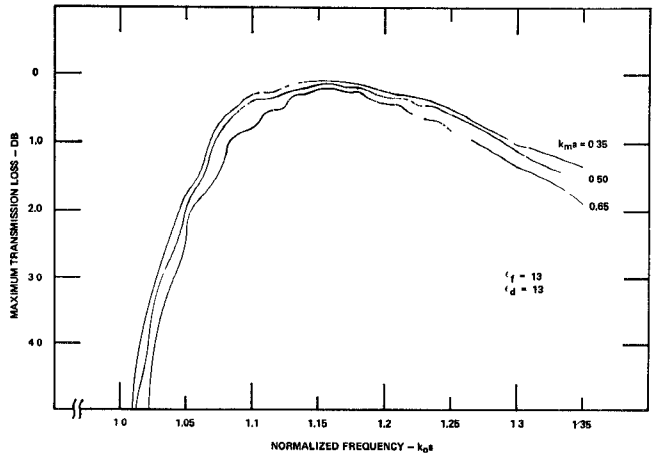

Fig. 8. Maximum transmission loss as a function of normalized frequency for various ferrites.

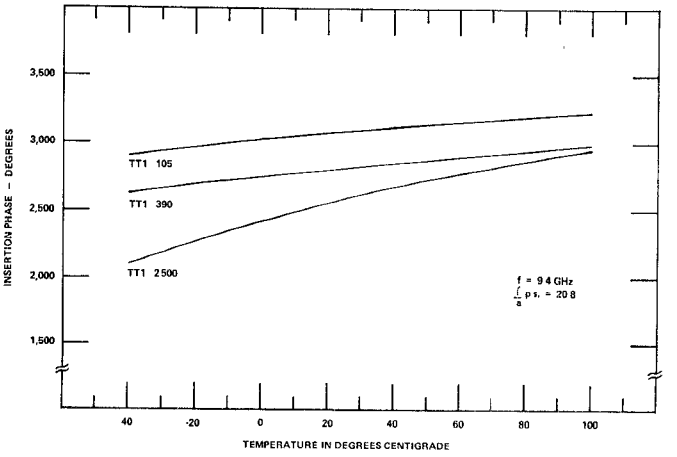

Fig. 10. Theoretical insertion phase variation with temperature at $f=9.4$ GHz.

assuming a perfectly square waveguide. Practical phase shifters will have manufacturing tolerances and errors which must also be considered in the loss analysis. Errors in the total length of the device contribute primarily to its insertion phase and can be limited to less than $\pm 10°$ between units without stringent manufacturing tolerances ($\Delta L \leq 0.005$ in).

The transmission loss of the phase shifter is quite sensitive to the waveguide aspect ration a/a'. As shown in the Appendix, the normal modes of the ferrite-loaded waveguide become elliptically polarized when this aspect ratio deviates from unity. In order to assess this effect, theoretical calculations were made for various aspect ratios. In the analysis this error is assumed to be constant along with the length of the phase shifter. Fig. 9 gives the frequency variation of the rotational losses for various values of aspect ratio over a 10-percent frequency band. From these curves it is seen that the aspect ratio must be closely controlled in order to reduce excess rotational losses. This is the most severe manufacturing tolerance on the phase shifter. Experimental data have verified these results.

IV. Temperature and Power Characteristics

The material property which determines the temperature and power-handling characteristics of the phase shifter is the saturation magnetization of the ferrite. As temperature increases, the saturation magnetization decreases, resulting in a decrease of differential phase shift and an increase in insertion phase. Using published data [20] for the change in $4\pi M_s$ with temperature, the effective permeability as given by (3) was calculated, and its effect on the variation on insertion phase is shown theoretically in Fig. 10 as a function of temperature. Thus phase shifters using high values of $4\pi M_s$ will be quite temperature sensitive. This is another consideration in the choice of ferrite material. At X-band measurements on a 360° phase shifter made from TT1-390 show a temperature sensitivity of about 3° insertion-phase increase per degree Celsius. This is in good agreement with the theoretical results shown in Fig. 10. (Also see [17].)

Theoretical and experimental results show that the differential phase shift is not a sensitive function of temperature. The principal mechanism, which reduces

the differential phase shift, is a reduction in the off-diagonal elements of the Polder tensor. The transmission loss of the phase shifter is insensitive to temperature until rotational losses caused by changes in ω_m/ω become significant. Low-power tests indicate that the transmission loss remains constant up to ambient temperatures of 100°C.

The ambient temperature of the phase shifter is determined by the heat input due to its loss and by the temperature of the heat sink to which it is connected. At high average-power levels, the increase in phase-shifter temperature causes a large rotational loss. This power is absorbed in the output linear polarizer and, if the thermal capacity of this polarizer is exceeded, results in device failure. The average power required to induce failure thus depends on low-power insertion loss, method of cooling, and the dissipation rating of the polarizer. Test results at X band have demonstrated operation above 150 W of average power with forced air cooling.

The peak-power handling capability of the phase shifter is determined by the onset of spin-wave instabilities and increases as ω_m/ω decreases. High-power tests at X band on the experimental phase shifters show this limit to occur at 1 kW for $\omega_m/\omega = 0.67$. Specially designed high-power phase shifters of this type have been reported [21] with peak-power handling capability in excess of 100 kW.

V. Discussion

An analysis of reciprocal Faraday-rotation ferrite phase shifters of square cross section has been presented and experimentally substantiated. This analysis provides a systematic approach to the design of wide-band high-performance phase shifters. The experimental direct-plated devices had a 1.3-dB insertion loss at X band and a 1.7-dB insertion loss at K_u band, both over a 10-percent frequency band, with over 360° of linear phase shift. In general this technique yielded attenuation factors of about 0.2 dB/in at X band and 0.3 dB/in at K_u band for the phase shifter. The geometry is convenient for latched operation and for efficient cooling. An error analysis has shown that one limitation to this approach is the stringent manufacturing tolerances on the aspect ratio of the waveguide.

The analysis also makes evident the tradeoffs available based on the choice of ferrite. All of the performance characteristics of the phase shifter are enhanced by the use of a low-saturation magnetization ferrite with the single exception of length and thus total transmission loss. The data presented here make it possible to choose an appropriate value of $4\pi M_s$ for a given application.

Appendix

Normal Modes of Nearly Square Waveguides

The normal modes of a longitudinally magnetized ferrite-filled square waveguide are right and left circularly polarized modes with propagation constants given by (7) and (8). In the case of the nearly square waveguide, the height (a') and the width (a) differ slightly. From [9] the normal modes of propagation satisfy the following transmission line equations:

$$\frac{1}{\beta_{01}^2}\frac{d^2I_{10}}{dz^2} = -\mu(I_{10} - jkI_{01}) \tag{29}$$

$$\frac{1}{\beta_{02}^2}\frac{d^2I_{01}}{dz^2} = \mu(jkI_{10} + I_{01}) \tag{30}$$

where

$$\beta_{01} = \omega\sqrt{\mu_0\epsilon_0\mu_r\epsilon_f}\left[1 - \left(\frac{\omega_{c1}}{\omega}\right)^2\right]^{1/2} \tag{31}$$

$$\beta_{02} = \omega\sqrt{\mu_0\epsilon_0\mu_r\epsilon_f}\left[1 - \left(\frac{\omega_{c2}}{\omega}\right)^2\right]^{1/2} \tag{32}$$

$$\omega_{c1} = \frac{\pi}{a\sqrt{\mu_r\epsilon_f\mu_0\epsilon_0}} \tag{33}$$

$$\omega_{c2} = \frac{\pi}{a'\sqrt{\mu_r\epsilon_f\mu_0\epsilon_0}} \tag{34}$$

$$k = \frac{-8}{\pi^2}\frac{\kappa}{\mu}. \tag{35}$$

Here β_{01} is the unperturbed propagation constant of the TE_{10} mode and β_{02} is the unperturbed propagation constant of the cross-polarized TE_{01} mode in the waveguide. Assuming solutions of the form

$$I_{10} = I_0 e^{-j\beta z} \tag{36}$$

$$I_{01} = I_0' e^{-j\beta z} \tag{37}$$

and substituting these in (29) and (30) gives

$$\frac{I_0}{I_0'} = \frac{-j}{2}\left[\frac{\xi}{k} \pm \sqrt{\left(\frac{\xi}{k}\right)^2 + 4(1+\xi)}\right] \tag{38}$$

where

$$\xi = \frac{\beta_{01}^2}{\beta_{02}^2} - 1. \tag{39}$$

Here, I_0 and I_0' represent the transverse magnetic field intensities for the TE_{10} and TE_{01} modes in the nearly square waveguide. Since from (38) the modes are in time quadrature, and since the magnitude of the amplitude ratio is, in general, different from unity, it is concluded from (38) that the normal modes in the nearly square waveguide ($\xi \approx 0$) are elliptically polarized, with the + and − giving opposite senses of elliptic polarization.

The ellipticity of these normal modes vary with waveguide aspect ratio, frequency, and ferrite magnetization and is plotted in Fig. 11 for various aspect ratios (a'/a) and a particular saturated ferrite. Notice that the ellipticity is different for the two senses of polarization.

The propagation constants of the normal modes in the nearly square waveguide can be found from the

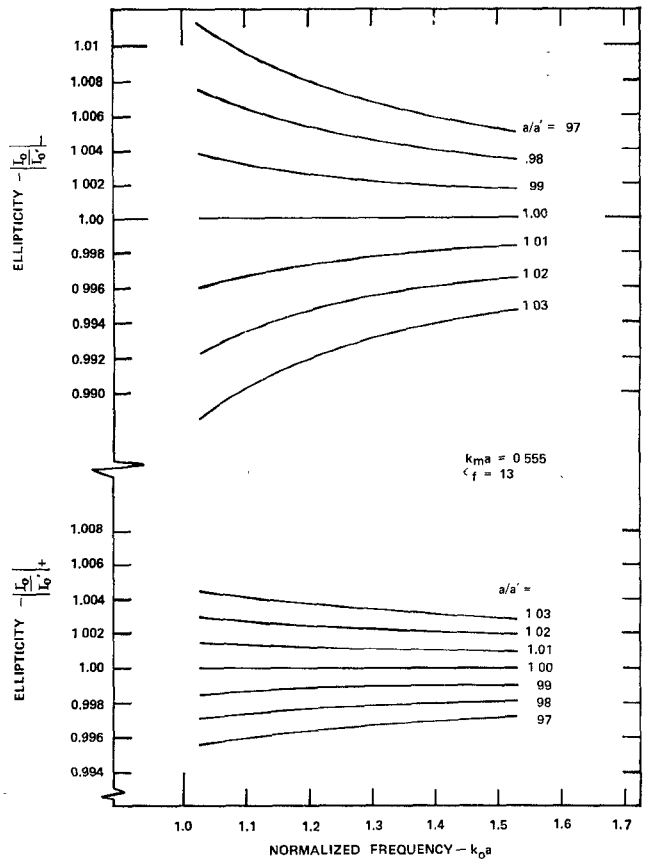

Fig. 11. Normal mode ellipticity versus normalized frequency for various waveguide aspect ratios (a/a').

solution of (29) and (30) with the result

$$\frac{\beta^2}{\beta_{01}{}^2} = \left[\frac{(2+\xi) \pm \sqrt{(2+\xi)^2 - 4(1+\xi)(1-k^2)}}{2(1+\xi)}\right]. \quad (40)$$

The ellipticity and the altered propagation constants in the nearly square waveguide degrades phase-shifter performance by introducing additional rotational errors and hence transmission loss.

References

[1] N. G. Sakiotis and H. N. Chait, "Ferrite at microwaves," *Proc. IRE*, vol. 41, Jan. 1953, pp. 87–93.

[2] H. N. Chait, "Nonreciprocal microwave components," in *1954 IRE Conf. Rec.*, pt. 8, pp. 82–87.

[3] B. Lax, K. J. Button, and L. M. Roth, "Ferrite phase shifters in rectangular waveguide," *J. Appl. Phys.*, vol. 25, Nov. 1954, pp. 1413–1421.

[4] A. G. Fox, S. E. Miller, and M. T. Weiss, "Behavior and applications of ferrite in the microwave region," *Bell Syst. Tech. J.*, vol. 34, Jan. 1955, pp. 5–103.

[5] N. G. Sakiotis, A. J. Simmons, and H. N. Chait, "Microwave-antenna ferrite applications," *Electronics*, June 1952, p. 156.

[6] H. Scharfman, "Three new ferrite phase shifters," *Proc. IRE*, vol. 44, Oct. 1956, pp. 1456–1459.

[7] F. Reggia and E. G. Spencer, "A new technique in ferrite phase shifting for beam scanning of microwave antennas," *Proc. IRE*, vol. 45, Nov. 1957, pp. 1510–1517.

[8] W. E. Hord and F. J. Rosenbaum, "Approximation technique for dielectric loaded waveguides," *IEEE Trans. Microwave Theory Tech.*, vol. MTT-16, Apr. 1968, pp. 228–233.

[9] ——, "Propagation in a longitudinally magnetized ferrite-filled square waveguide," *IEEE Trans. Microwave Theory Tech. (Corresp.)*, vol. MTT-16, Nov. 1968, pp. 967–969.

[10] W. E. Hord, F. J. Rosenbaum, and C. R. Boyd, "Theory of the suppressed-rotation reciprocal ferrite phase shifter," *IEEE Trans. Microwave Theory Tech.*, vol. MTT-16, Nov. 1968, pp. 902–910.

[11] D. Polder, "On the theory of ferrimagnetic resonance," *Phil. Mag.*, vol. 40, 1949, p. 99.

[12] W. E. Hord, C. R. Boyd, and F. J. Rosenbaum, "Application of reciprocal latching ferrite phase shifters to lightweight electronic scanned phased arrays," *Proc. IEEE*, vol. 56, Nov. 1968, pp. 1931–1939.

[13] E. Schlömann, "Microwave behavior of partially magnetized ferrites," *J. Appl. Phys.*, vol. 41, Jan. 1970, pp. 204–214.

[14] B. Lax and K. J. Button, *Microwave Ferrites and Ferrimagnetics*. New York: McGraw-Hill, 1962, p. 298.

[15] H. K. F. Severin, "Propagation constants of circular cylindrical waveguides containing ferrites," *IRE Trans. Microwave Theory Tech.*, vol. MTT-7, July 1959, pp. 337–346.

[16] C. R. Boyd, Jr., "A dual-mode latching, reciprocal ferrite phase shifter," in *1970 Int. Microwave Symp. Dig.*, pp. 337–340; IEEE Cat. No. 70C10-MTT.

[17] R. G. Roberts, "An X-band reciprocal latching Faraday rotator phase shifter," in *1970 Int. Microwave Symp. Dig.*, pp. 341–345; IEEE Cat. No. 70C10-MTT.

[18] A. G. Gurevich, *Ferrites at Microwave Frequencies*. Cambridge, Mass.: Boston Tech. Pub., Inc., 1965, pp. 161–166.

[19] M. L. Reuss, Jr., "A nonreciprocal circular polarizer," *IEEE Trans. Microwave Theory Tech.*, vol. MTT-15, Jan. 1967, pp. 37–41.

[20] *Trans-Tech Catalog*. Gaithersburg, Md.: Trans-Tech, Inc.

[21] C. R. Boyd, Jr., L. R. Whicker, and R. W. Jansen, "An S-band, dual mode reciprocal ferrite phase for use at high power levels," in *1970 Int. Microwave Symp. Dig.*, pp. 346–350; IEEE Cat. no. 70C10-MTT.